NUREG/CR-3845
LA-10090-MS

Los Alamos National Laboratory is operated by the University of California for the United States Department of Energy under contract W-7405-ENG-36.

Prediction of Nonlinear Structural Response in LMFBR Elevated-Temperature Piping

Los Alamos National Laboratory
Los Alamos, New Mexico 87545

Prepared by Pauline Lujan, Group Q-13

NUREG/CR-3845
LA-10090-MS

R7

Prediction of Nonlinear Structural Response in LMFBR Elevated-Temperature Piping

Charles Farrar

Manuscript submitted: March 1984
Date published: June 1984

Prepared for
Severe Accident Assessment Branch
Division of Accident Evaluation
Office of Nuclear Reactor Research
US Nuclear Regulatory Commission
Washington, DC 20555

NRC FIN No. A7242

Los Alamos National Laboratory
Los Alamos, New Mexico 87545

PREDICTION OF NONLINEAR STRUCTURAL RESPONSE IN LMFBR ELEVATED-TEMPERATURE PIPING

by

Charles Farrar

ABSTRACT

The development of structural analysis capabilities to investigate possible accident initiations caused by structural degradation of liquid metal fast breeder reactor (LMFBR) piping is summarized. The ABAQUS finite element code is used to perform a nonlinear analysis of a bench mark problem proposed by the Pressure Vessel Research Committee. The problem is representative both in geometry and loading of an LMFBR elevated-temperature piping system, and published analytical results are available for comparison. Results show the system to be most sensitive to large, radial, thermal gradients that occur when the system experiences certain thermal transients. Repeated cycles of these transients will lead to thermal ratcheting, causing progressive deformation and strain accumulation in the system. Future work will verify the accuracy of the finite element model and quantify damage accumulated during the lifetime of an LMFBR elevated-temperature piping system.

I. INTRODUCTION

This report summarizes the structural analysis capabilities currently being developed by the Los Alamos National Laboratory for the Office of Nuclear Regulatory Research's Accident Initiation From Component Structural Degradation program. To date these capabilities have focused on the use of the finite element code ABAQUS[1] and its ability to model complex piping systems. The code is being used to determine the nonlinear response of a typical hot leg of

the primary heat transport system (PHTS) sodium loop in a liquid metal fast breeder reactor (LMFBR). The response is caused by the loads specified in a histogram developed by the Clinch River Breeder Reactor (CRBR) designers which envelops all the expected normal, upset, and emergency load conditions throughout the 30-year operating life of the system.[2] The load histogram includes effects of gravity, internal pressure, thermal transients including creep-hold time, and differential movement of the end boundaries during temperature variations.

This particular piping system and load history are the subject of a bench mark problem for the Pressure Vessel Research Committee's (PVRC) project, Comparative Studies on High-Temperature Piping. Several independently published studies of the problem that utilize different finite element codes, as well as different modeling techniques within ABAQUS, provide analytical results with which the preliminary results of this investigation may be compared.[2,3,4]

Certain structural concerns were identified during the Nuclear Regulatory Commission's (NRC) review of the CRBR Preliminary Safety Analysis Report (PSAR). Of specific concern were component failures from material defects or material degradation that could initiate accidents jeopardizing containment integrity. The structural analysis capabilities developed during this investigation and the information obtained from subsequent application of these capabilities will provide data and the analytical techniques necessary for further detailed studies of these structural concerns in LMFBR elevated-temperature piping systems.

The PVRC bench mark problem is first presented and is then followed by a discussion of the results thus far obtained. Subsequently, an overview of the future work necessary to complete this portion of the program and an example of the application of this work to a specific structural concern are summarized.

II. PIPING-SYSTEM DESCRIPTION

The piping system currently being analyzed is identical to the portion of the CRBR's PHTS piping between the primary sodium pump and the intermediate heat exchanger (IHX) as shown in Figs. 1 and 2. This portion of the PHTS consists of 60.96-cm (24-in.) o.d., 316 stainless steel (SS), insulated pipe,

1.27 cm (0.5 in.) thick. The pipe is rigidly fixed to the vessels at each end and supported at intermediate locations, shown in Fig. 2, by five constant hanger supports. The seismic snubbers that exist on the actual piping system have been deleted in this initial investigation because the load histogram does not specify conditions which would cause their reactions to be significant. The operating temperature of the system is 546°C (1015°F), and the operating pressure is 1.16 MPa (168 psi).

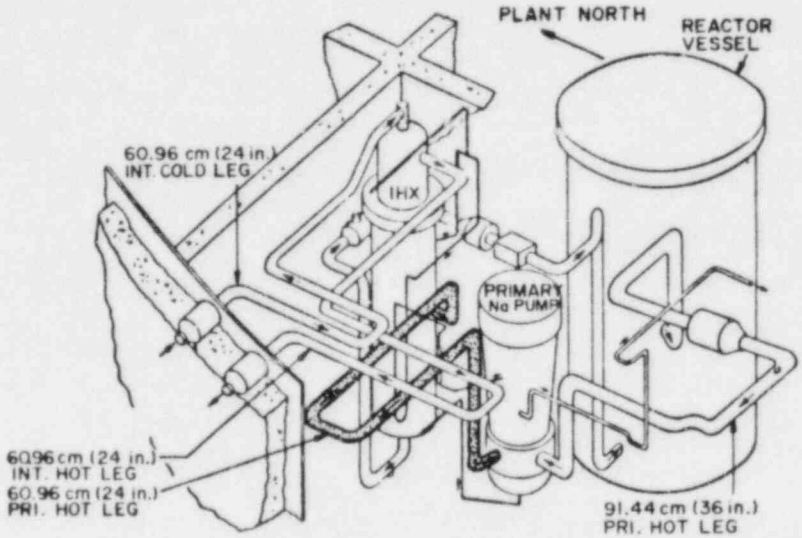

Fig. 1. Typical in-containment PHTS piping, highlighted section is the portion of the PHTS being analyzed in the PVRC bench mark problem.

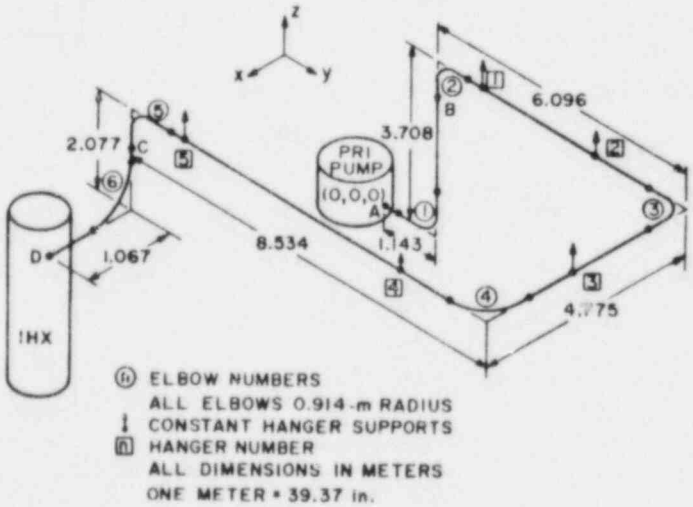

Fig. 2. The piping system that is analyzed in the PVRC bench mark problem.

III. LOAD HISTOGRAM

The load histogram is summarized in Table I. The initial step of the sequence is used to calculate the constant hanger reactions. The rest of the load histogram is intended to encompass the 863 possible thermal transient events identified by the reactor-plant designers. As stated earlier, these loadings cover all normal, upset, and emergency events postulated for the system. Load steps 1-18, set A, comprise the 36 most severe thermal downshock transients; set B envelops 36 moderately severe up-and-down thermal transient events. The last set, set C, contains the remainder: 791 less severe events.[2]

The pipe and pipebend elements of ABAQUS allow three temperatures to be specified through the thickness of the pipe. A previously performed heat-transfer analysis[5] provides the temperature distributions through the pipe thickness during the thermal transient events. Temperatures are assumed to be constant in the axial direction for the entire system.

Seismic loading is not treated explicitly in this analysis. Instead, the dead weight, constant hanger reactions, and internal pressure are increased to two or three times their value under normal operating conditions to account for possible seismic events occurring during the thermal transients.

When thermal transients occur, the IHX and primary sodium pump experience unequal thermal expansions and contractions. The loads induced in the pipe system by this differential end movement are incorporated into the analysis by specifying the end displacements as a function of temperature (Table II). For intermediate load steps added to simulate thermal gradients (that is, steps 4-18 of Table I), the end displacements are interpolated linearly for the pipe's middle-surface temperature. The load histogram neglects forces induced in the piping system by the sodium flow.

IV. FINITE ELEMENT MODEL

The piping system is modeled with the elbow elements of the ABAQUS finite element code. To model both the predominantly shell behavior of the pipe bends and the predominantly beam behavior of the straight segments with one type of element, the code considers the pipe as a beam with a deforming thin-walled

cross section and restricts the response to small displacements. This restriction allows the strains from shell and beam behavior to be analyzed separately and the results linearly superposed. The combination of shell and beam properties enables the elbow elements to accurately predict the response of the piping system to such effects as (1) increased stiffness from internal pressure, (2) increased flexibility from ovalization of an elbow, (3) the transition from shell behavior of an elbow to beam behavior of the adjacent straight segment, and (4) warping from curved beam bending and torsion of the ovalized section. A detailed summary of the properties of these elements and their formulation is available in Ref. 1.

The six elbows of the system being analyzed and, where geometrically possible, the adjacent 0.61 m (2 ft, 1 pipe diameter) of straight pipe are modeled with the Elbow31 element of the code. The straight portions are included to provide the shell/beam behavior-transition range mentioned above. The remaining straight portions of the pipe are modeled with the Elbow31B element. Whereas the Elbow31 element allows both ovalization and warping of the cross section and provides linear interpolation of these quantities in the axial direction, the Elbow31B element considers ovalization as the only possible cross-section deformation and neglects any axial gradient in this quantity. The ovalization in the Elbow31B elements is constrained to uniform radial expansion to model the effects of internal pressure on the straight segment of pipe away from the elbows. The degree to which the system is discretized is based on the comparison of the results of several trial analyses with the results of published analyses.

To maintain continuity, boundary conditions must be specified at the interface between Elbow31 and Elbow31B elements. Both warping and ovalization must be constrained in the Elbow31 element at this point, reducing all cross-sectional deformations to uniform radial expansion. The user, therefore, specifies the transition point from shell to beam behavior. The ovalization and warping are also constrained at the ends of the system where the pipe intersects the IHX and primary sodium pump. The pipe/vessel connections are both modeled as rigid, and the nozzle stiffness at these locations is neglected. The constant hanger supports are assumed to be axial members only, and any rotational restraints imposed by the hangers are neglected.

The material properties used in the analysis are summarized in Tables III and IV.[5] Environmental effects on material properties (such as irradiation,

thermal aging, and corrosion, etc.) have been neglected. A kinematic hardening law is used, and the stress-strain curve is idealized as bilinear according to the procedure outlined in Ref. 6.

The location of a point at which a variable is calculated is given by the element number, integration point (IP), and section point (SP). The elements are numbers sequentially beginning at the primary sodium pump. Element n runs from node n to node n+1. The node-numbering system is shown in Fig. 3. The IP specifies the location circumferentially: as one views a cross section of element n, looking from node n+1 towards node n, IP 1 is located on the intrados of the elbow, and the rest of the IPs are located sequentially in a counterclockwise direction at uniform increments. For straight runs, IP 1 is located at the intrados of the previous elbow, except for elements one and two that use the elbow immediately following. The SP locates the point of interest radially, with SP 1 specifying the inside surface. The remaining SPs are numbered sequentially in the outward radial direction.

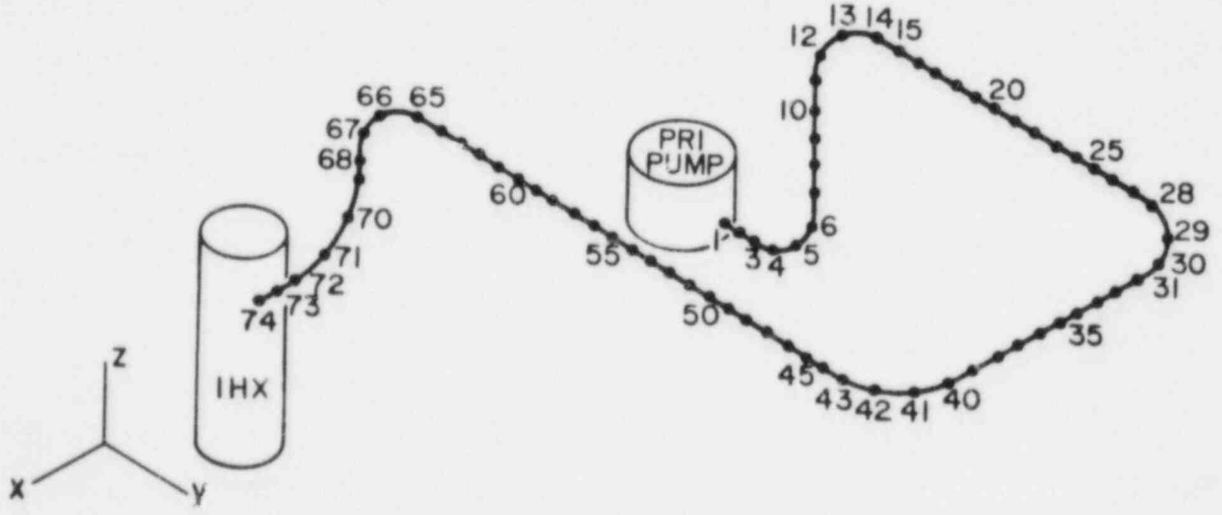

Fig. 3. The node-numbering system used in the finite element model of the PVRC bench mark problem.

V. RESULTS

Postprocessing subroutines have been developed to provide graphical displays of the results. The displays fall into two categories: profile plots that, for a particular load step, show the circumferential distributions of a variable at a cross section in the piping system and history plots that describe the change in a particular variable over the entire load history. The following examples, Figs. 4 through 8, show von Mises equivalent stress defined as

$$\bar{\sigma}^2 = 3/2\ \sigma'_{ij}\ \sigma'_{ij} \quad ,$$

$$\sigma'_{ij} = \sigma_{ij} - (\sigma_{kk}\ \delta_{ij})/3 \quad ,$$

where

$\bar{\sigma}$ = von Mises equivalent stress,

σ'_{ij} = deviatoric stress tensor, and

σ_{ij} = stress tensor,

plotted either in profile or history form. The postprocessing capabilities are not limited tc this quantity, as is evident in Fig. 9, and the subroutines may be easily modified to plot any variable calculated by ABAQUS. In the following discussion, load steps refer to those outlined in Table I, equivalent stress refers to von Mises equivalent stress, elbow numbers and hanger numbers refer to those designated in Fig. 2, and the terms load increment and time increment are used interchangeably. For loads applied instantaneously (as an example, load step 1), the load increments represent a fictitious time increment, the entire load step requiring one time unit. In load step 2, the load increments correspond to portions of the actual creep-hold time. The node-numbering system, element-numbering system, and the reference system used to locate the integration points and section points are outlined in the previous section.

The graph shown in Fig. 4 provides a three-dimensional time history of the maximum equivalent stress calculated for each element during the first two load steps. The load increments corresponding to the creep-hold time (increments 7-99) do not represent uniform time increments because ABAQUS automatically

increases the time interval incrementally while integrating the creep-strain-rate equation. Because the size of the increments is based on stability criteria for ABAQUS's integration scheme, there is no guarantee that a uniform increment will be selected.

Figures 5a-c show a time history of the equivalent stress for a particular location in elbow 5. This plot is similar to one that would be obtained by passing a plane through Fig. 4 parallel to the equivalent stress-load increment plane.

A cross section of Fig. 3 may be taken parallel to the equivalent-stress element number plane as shown in Figs. 6 and 7. In these plots the right-hand axis, together with the •'s and triangles, locates the point in the element at which the maximum equivalent stress occurs.

Figures 8 and 9 are examples of profile plots of equivalent stress and hoop strain. Both these plots are of a cross section in elbow 5 located 45^{o} from node 68.

The results of load step i are summarized in Table V. Except for hanger 1, the values obtained in this investigation appear to be very consistent with those of the previously published analyses.

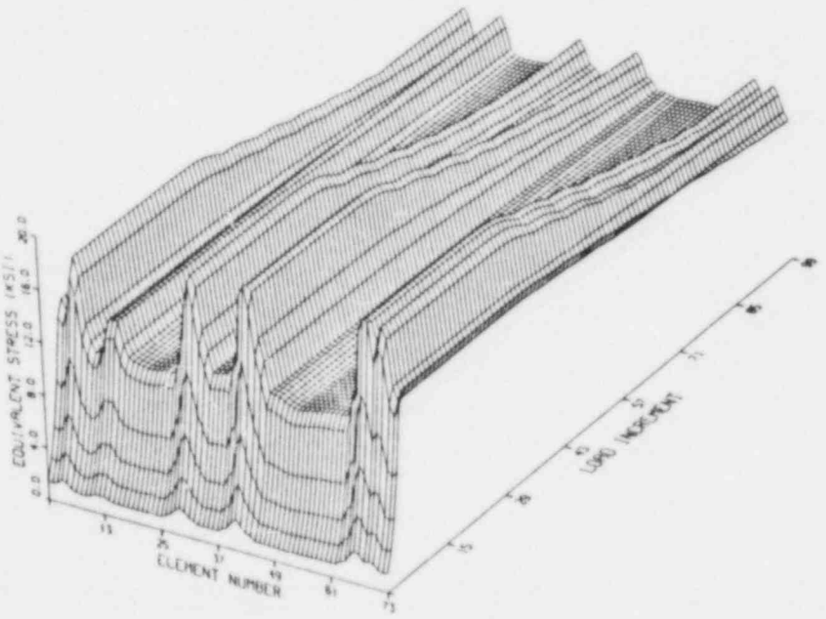

Fig. 4. Maximum von Mises equivalent stress calculated for each element during the first two load steps of Table I.

The PISAC and PINA analyses prescribe stiffness values at the vessel/pipe interface as opposed to the completely rigid boundary conditions used in this investigation. The elbow elements available in the MARC code provide constant ovalization without warping and neglect the axial stresses caused by internal pressure.[2] These differences are possible sources of the discrepancy at hanger 1; however, without further details concerning the actual finite element models used, pinpointing the source of the discrepancy will be difficult. Hanger 1 appears to be a sensitive area in the system, as discrepancies exist among all the models.

Because an elbow behaves like a shell, bending causes the cross section to ovalize, which in turn reduces the flexural rigidity of the system. In the presence of bending caused by thermal loads, the system deformations will tend to be concentrated at the elbows; the concentration of deformation, which results from shell behavior, causes higher stresses and strains at these locations. Figures 4, 6, and 7 depict the equivalent-stress level in the piping system when the system is exposed to bending from thermal loads. As expected, six distinct peaks in the equivalent-stress plots occur at locations corresponding to the six elbows of the system. The peaks are maintained throughout the portion of the load histogram that has been analyzed. The location of the maximum equivalent stress varies from elbow 4 to elbow 5. These maximums do not correspond to elbows 1 and 6 as reported in Refs. 1 and 2, but they do correspond to a recent unpublished analysis independent of this investigation.[7]

The effects of creep can be seen in Figs. 4, 5b, and 6-9. Most apparent in Figs. 4, 6, and 7 is the strong dependence of the equation representing creep-strain rate on the equivalent-stress level. The rate of stress relaxation is a function of the creep-strain rate which, in turn, is a function of the equivalent stress and temperature. When the temperature is held constant in load step 2, the rate of relaxation is greatest at the locations where the equivalent stress is greatest, that is, the elbows. In the straight runs of pipe where the equivalent stress is less, the relaxation is undiscernible. The peak equivalent stresses shown in Fig. 5 reduce to an almost uniform value at the end of the creep-hold time, shown in Fig. 6, as would be expected from the stress-level dependence of the creep-strain rate. Figure 8 shows the local redistribution in the stress level around the inside circumference of element 66. Figure 9 shows the local relaxation in elastic hoop strain around the inside circumference of element 66.

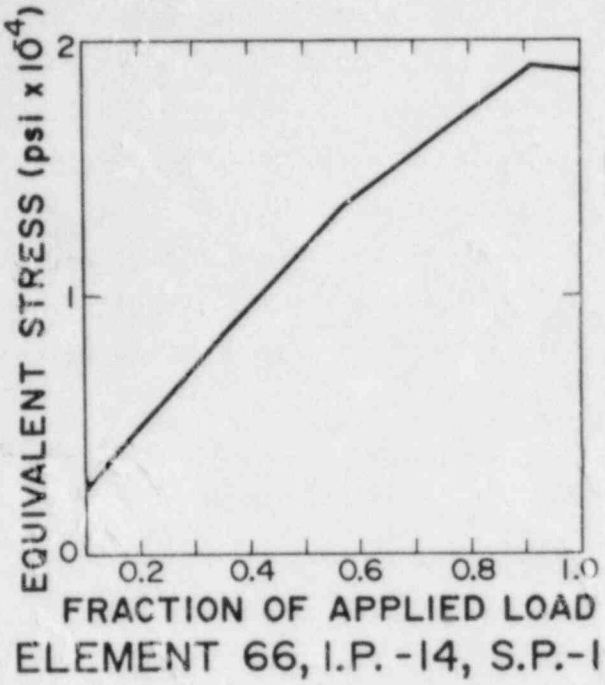

Fig. 5a. The von Mises equivalent stress vs fraction of applied load, Step 1 of Table I.

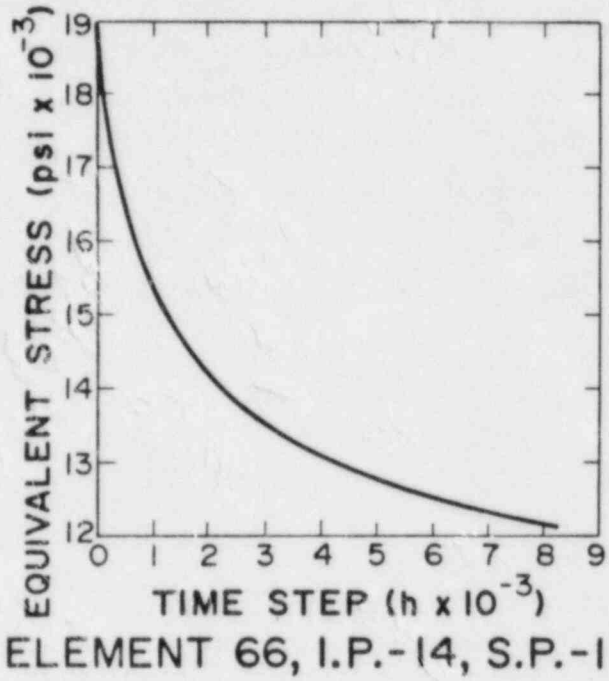

Fig. 5b. The von Mises equivalent stress creep-hold time, Step 2 of Table I.

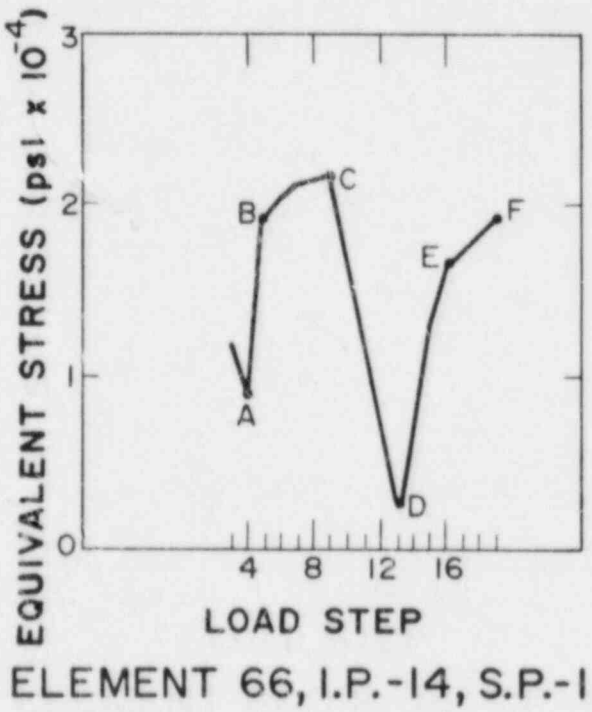

Fig. 5c. The von Mises equivalent stress vs load step, Steps 3 through 18 of Table I.

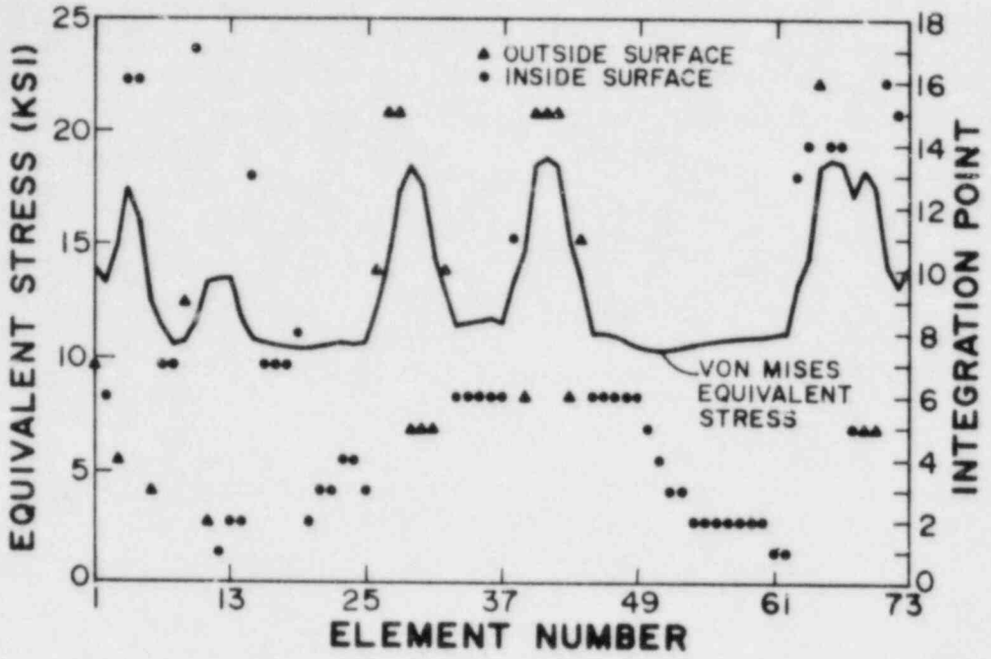

Fig. 6. Maximum von Mises equivalent stress at the beginning of creep-hold time and the location within each element at which the maximum occurs.

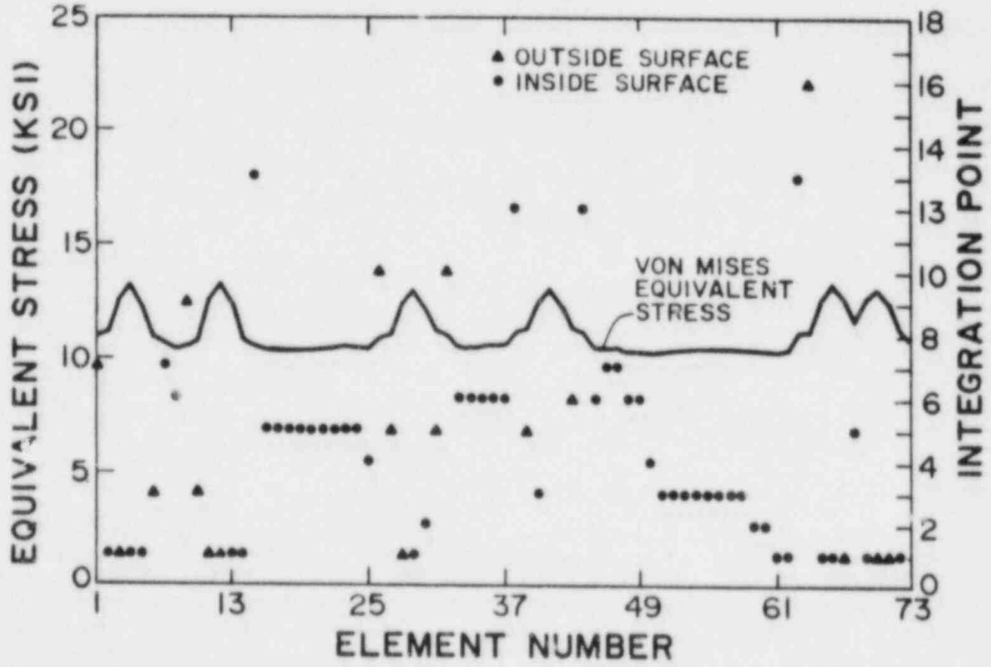

Fig. 7. Maximum von Mises equivalent stress at the end of creep-hold time and the location within each element at which the maximum occurs.

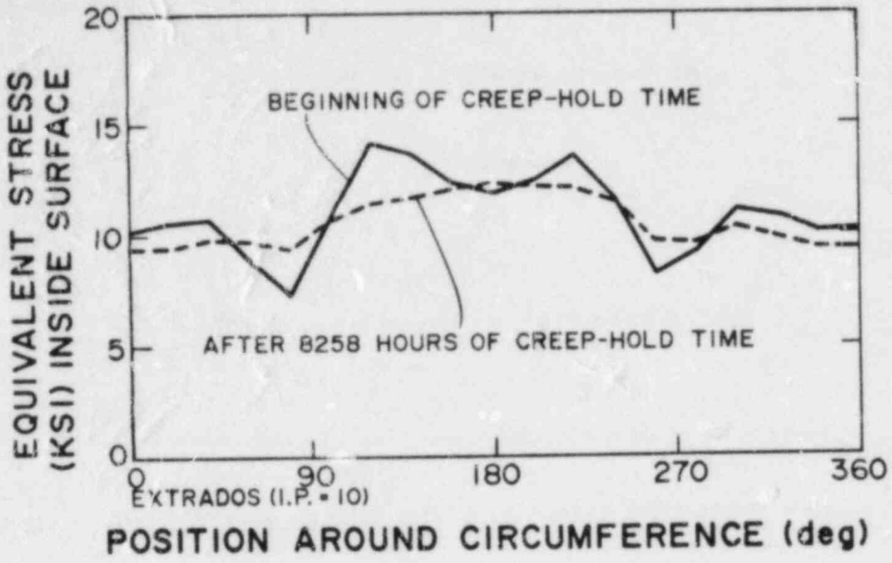

Fig. 8. Circumferential variation of von Mises equivalent stress on the inside surface of elbow 5.

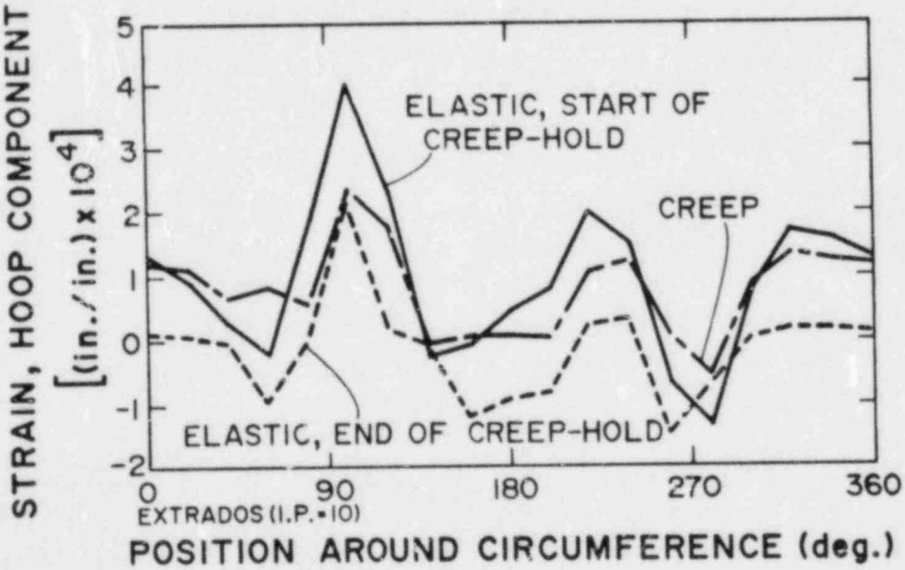

Fig. 9. Circumferential variation of hoop strain on the inside surface on elbow 5.

Figure 5c is a plot of the effective-stress history for one integration point in the most highly stressed element during the first thermal downshock, load steps 4-18. The CRBR plant designers have postulated a drop in pressure preceding each thermal downshock, and point A in the plot corresponds to the reduction in equivalent stress associated with this drop in pressure of 1.16 MPa (168 psi).

Initially, as the system cools down (points A-C), a large radial thermal gradient is developed. At point B, the particular location on the elbow for which the plot was made begins to yield with both the hoop and axial stresses in tension. The system continues to yield until the maximum radial gradient of 54.9°C (130°F) is reached (point C). During this portion of the load history, the tensile stresses on the inside surface of pipe are the result of the radial gradient caused by the different rates at which the inside and outside surfaces are cooling. The inside surface cools more rapidly, but the corresponding contraction is restricted by the slower cooling outside surfaces. As the temperature is cycled through the load history, these large radial thermal gradients will set up a thermal ratcheting mechanism resulting in progressive deformation of the section and strain accumulation. As the thermal gradient decreases (points C-F), this location on the inside surface of the pipe unloads elastically, and eventually both the hoop and axial components of the stress go into compression at point D. A continued drop in the system temperature and a reduction in the radial gradient cause yielding at point E, but this time the yielding is caused by compressive stresses. Note that the effective-stress value at point E, corresponding to yielding in compression, is less than the effective-stress value at point B, corresponding to the initial yielding in tension. This would be expected from the kinematic shift in the yield surface. The severe effects of the large radial thermal gradients are most noticeable in the group of plots, Figs. 5a-c. The maximum stress found during the portion of the load history that has been analyzed occurs at point C, when the thermal gradients reach a peak, even though both temperature and pressure are significantly reduced from their previous maximums that occurred at the end of load step 1.

VI. FUTURE WORK

Structural analysis capabilities will continue to be developed through further studies of the PVRC bench mark problem. The original intent of this work was to provide a standard problem, conservatively representative of an elevated-temperature piping system, with which the analytical results of different finite element codes could be compared. This problem incorporates several idealizations and simplifications into both the geometric and material models (as well as the load histogram) that do not accurately represent a typical LMFBR elevated-temperature piping system or its typical loading. In its present form, the problem is useful in developing analytical capabilities. However, to be useful in future investigations of actual structural concerns, certain modifications must be made, including alterations to the load histogram and changes to the material model. In addition, several topics relating to the mechanics of piping systems, finite element modeling, and material behavior in an elevated-temperature environment must be addressed to verify the accuracy of the results obtained during this investigation. These topics include examining the boundary conditions of the vessel/pipe interface, developing structural dynamic analysis capabilities, determining the location of the shell behavior/beam behavior transition point, and reviewing current literature to determine how the long-term exposure to an elevated-temperature, radioactive sodium environment will affect stainless steel material properties and, in turn, how these effects might change the piping-system response.

The development of dynamic analysis capabilities is necessary to determine the validity of using equivalent static loads to approximate the effects of seismic events occurring during a thermal transient. These capabilities will also be used to approximate the effects of deleting the seismic snubbers from the system model. Dynamic analysis may also be needed to accurately predict the strain accumulation in a component, as the equivalent static loads used in the PVRC bench mark problem appear to be overly conservative in this respect.

Currently the vessel/pipe interface is being modeled as a completely rigid connection. Other investigations have stiffness values for certain degrees of freedom incorporated into the boundary conditions. An investigation into the magnitude of these values and their effect on the system response will be necessary to determine if the simplification used in this analysis is justified.

The location of the shell behavior/beam behavior transition point is a parameter to which the response of the system is quite sensitive. At this time the location of the point is determined through a trial-and-error process. Computer costs are needlessly escalated if the point is located too far into the beam-response range, because the additional integration points required to model the insignificant shell behavior in this region rapidly increase the computer time needed to solve the problem. If the point is located too close to the elbow, significant ovalization in the adjacent straight run may be neglected and the accuracy of the response adversely affected. Guidelines will be established, stated in terms of pipe geometry and based on the mechanics of the elbow/straight pipe transition, by which the location of the transition point may be more easily determined.

The PVRC bench mark problem considers the piping system to be a uniform, continuous piece of pipe. An actual system will have welded joints, and residual stresses caused by the welding process will be present. These residual stresses (if significant) must be quantified and incorporated into the analysis.

As a final step in this analysis procedure, methods of extrapolating the data obtained from the analysis of a load histogram (similar to that outlined in Table I) to the entire operating life of the plant must be developed to determine strain accumulation in components and approximate future stress levels in components.

Further investigation of the constitutive model will focus on the Oak Ridge National Laboratory (ORNL) constitutive theory for stainless steel. This constitutive model, as incorporated in ABAQUS, is summarized in Ref. 1, and a summary of the research on which it is based is available in Ref. 8. Briefly, the theory decomposes the total strain into elastic response, rate-independent plastic response, and rate-dependent creep response, each being governed by a separate constitutive relationship. The equations representing the different constitutive relationships are coupled to model the experimentally observed dependence of the response on prior deformation, stress, and temperature.[8]

In addition to comparing the results of the PVRC bench mark problems with published computer solutions, analytical results should be compared with experimental data. This will require loading and response data to be obtained

from an experimental test facility which monitors a piping system that includes primary features (material, loading, temperature) of the system analyzed in this investigation. The test system will be modeled with ABAQUS to establish a correlation between an actual measured response and the response predicted by a finite element analysis. If applicable experimental data cannot be found, a testing program will be proposed.

The goal of this portion of the Accident Initiation From Component Structural Degradation program is to apply the analytical techniques and an understanding of elevated-temperature LMFBR piping behavior to specific structural concerns related to the program. One example of a structural concern where these capabilities may be applied, and which has already been identified as a concern by the NRC's review of the CRBR's PSAR, is leak-before-break assurance. This application may require modifications to the ABAQUS code so that the effects of a crack on the piping-system stiffness may be modeled indirectly (currently ABAQUS has no direct means of modeling this effect). The local stress field around the crack will be determined and used as a boundary condition in a subsequent fracture analysis. The fracture analysis will then determine if, under possible loading conditions, a flaw will continue to grow through the piping wall before it lengthens enough to cause either stable or unstable crack growth.

VII. SUMMARY

The nonlinear analysis capabilities of the ABAQUS finite element code have been used to model the response of a typical LMFBR elevated-temperature piping system subjected to normal, upset, and emergency loads. The results obtained thus far show that the radial thermal gradients caused by the first thermal downshock outlined in Table I produce the most severe stress levels experienced by the system. Repeated cycles of similar thermal transients will produce thermal ratcheting, leading to progressive deformation and strain accumulation. A comparison with experimental results has not yet been made, and verification of the analytical results is currently based on comparison with the other published[2,3,4] and unpublished[7] analytical results.

The investigation of this problem, which was originally proposed as a bench mark problem by the Pressure Vessel Research Committee, has enabled Los Alamos

National Laboratory to develop the capabilities necessary to model the response of elevated-temperature piping systems. However, this investigation has also led to several currently unresolved questions regarding finite element modeling of piping systems, material models for stainless steel, and thermal/mechanical response mechanisms. Future work will involve resolving these questions, modifying the structural model and load histories currently being used to make them more representative of typical LMFBR elevated-temperature piping systems, and applying the analytical techniques developed during the investigation to the study of specific structural concerns.

REFERENCES

1. ABAQUS Computer Program Manuals (Hibbitt, Karlsson & Sorensen, Inc., Providence, Rhode Island, 1981), Vols. 1-4.

2. A. K. Dhalla, "A Procedure to Evaluate Structural Adequacy of a Piping System in Creep Range," in Benchmark Problem Studies and Piping System at Elevated Temperature, F. L. Cho, R. L. Roche, Y. Yamada, Eds., PVP Conf., Orlando, Florida, June 27-July 2, 1982 (ASME, New York, 1982), PVP-Vol. 66, pp. 47-59.

3. A. K. Dhalla, H. D. Hibbitt, and E. K. Leong, "Detailed Inelastic Analysis of an LMFBR Pipeline," in Benchmark Problem Studies and Piping System at Elevated Temperature, F. L. Cho, R. L. Roche, Y. Yamada, Eds., PVP Conf., Orlando, Florida, June 27-July 2, 1982 (ASME, New York, 1982), PVP-Vol. 66, pp. 61-76.

4. O. Watambe, H. Ohtsubo, K. Yamazato, A Imazo, and H. Shoji, "Inelastic Analysis of Complex Piping Systems in Elevated Temperature Environment by Simplified Methods," in Benchmark Problem Studies and Piping System at Elevated Temperature, F. L. Cho, R. L. Roche, Y. Yamada, Eds., PVP Conf., Orlando, Florida, June 27-July 2, 1982 (ASME, New York 1982), PVP-Vol. 66, pp. 77-93.

5. A. K. Dhalla, Westinghouse Electric Corporation, letter to George Buchanan (March 2, 1983).

6. Nuclear Standard NE F9-5T, "Guidelines and Procedures for Design of Class 1 Elevated Temperature Nuclear System Components," U.S. Department of Energy (March, 1981).

7. E. P. Sorensen, Hibbitt, Karlsson, and Sorensen, Inc., letter to George Buchanan (June, 1983).

8. C. E. Pugh, "Progress in Developing Constitutive Equation for Inelastic Design Analysis," J. Pressure Vessel Technol., Vol. 105, pp. 273-276 (August, 1983).

TABLE I
LOAD HISTOGRAM

Set	Load Steps	Temperature Range[a]	Description[b]
A	i[c]	21.1	Set hanger forces: Pressure (1.16 MPa), dead weight,[d] at room temperature.
	1	21.1-546.	First heat-up transient: Increase pressure and dead weight to three times the value used in step i. Apply three times the constant hanger forces calculated in step i as concentrated forces at hanger locations. Increase temperature to system operating temperature.
	2	546.	Creep-hold time of 8258 hr.
	3	546.	Reduce pressure to 2.32 MPa.
	4-18[e]	546.-204.	First downshock transient.
B	f	204.-316.	Uniform temperature increase.
	f	316.-448.-316.	Second transient.
	f	316.	Increase pressure to 3.48 MPa.
	f	316.-546.	Third heat-up transient.
C	f	546.	Creep-hold time of 3258 hr.
	f	546.	Reduce pressure to 2.32 MPa.
	f	546.-204.	Third downshock transient.
	f	204.-21.1	Cool down to room temperature.

[a]All temperatures are given in degrees Celsius.

[b]Each description outlines only the changes from the previous description.

[c]This step is analyzed separately from the rest of the histogram to determine constant hanger forces.

[d]The dead weight of vertical runs (A-B, C-D, Fig. 2) equals 40.1 N/cm; the horizontal run (B-C, Fig. 2) equals 58.3 N/cm. This idealization accounts for increased dead weight on horizonal runs from the weight of the sodium and insulation.

[e]Multiple load steps are required to incorporate the nonuniform radial temperature distribution in the pipe during the transient.

[f]These are load sequences that have yet to be analyzed.

TABLE II
DISPLACEMENT OF THE PRIMARY SODIUM PUMP
AND IHX CAUSED BY THERMAL LOADING

Primary Sodium Pump

Direction[a]	Displacement[b]
Y	0.409 cm + 0.00249 cm/°C (T-204°)
Z	-1.29 cm - 0.00550 cm/°C (T-204°)

IHX

Direction[a]	Displacement[b]
X	-0.511 cm - 0.00317 cm/°C (T-204°)
Z	-2.05 cm - 0.0111 cm/°C (T-204°)

[a]Direction refers to coordinate system shown in Fig. 2.
[b]T = temperature at which displacement is sought in degrees Celsius ($204^{\circ} \leq T \leq 546^{\circ}$).

TABLE III
TEMPERATURE (T)-DEPENDENT ELASTIC AND PLASTIC MATERIAL
PROPERTIES FOR 316 SS PIPING MATERIAL

	English[a]
Modulus of Elasticity	= 28.9×10^{6} - 6850.0 (T-70) psi
Average Yield Stress[b]	= 23103.0 - 4.9925 (T-70) psi
Poisson's Ratio	= $0.2654 + 4.2688 \times 10^{-5}$ (T-70)
Coefficient of Instantaneous Thermal Expansion	= $9.062 \times 10^{-6} + 2.518 \times 10^{-9}$ (T-70) in./in./°F
Plastic Work-Hardening Slope[b,c]	= 1.365×10^{6} psi
	SI[d]
Modulus of Elasticity	= 199.3 - 0.08501 (T-21.1) GPa
Average Yield Stress[b]	= 159.3 - 0.06196 (T-21.1) MPa
Poisson's Ratio	= $0.2654 - 7.684 \times 10^{-5}$ (T-21.1)
Coefficient of Instantaneous Thermal Expansion	= $1.631 \times 10^{-5} + 8.158 \times 10^{-9}$ (T-21.1) cm/cm/°C
Plastic Work-Hardening Slope[b,c]	= 9.411 GPa

[a]All temperatures are in degrees Fahrenheit (°F).

[b]The average yield stress and plastic work-hardening slope are obtained from a bilinearized stress-strain curve with a maximum strain of 0.3%.

[c]The plastic work-hardening slope is defined as $\Delta \sigma / \Delta E_p$, where the stress increment beyond the yield point is divided by the plastic strain.

[d]All temperatures are in degrees Celsius (°C).

TABLE IV
TIME-DEPENDENT CREEP PROPERTIES FOR 316 SS PIPING MATERIAL

The equation for uniaxial creep strain (e_c) as a function of time (t), stress (σ), and temperature (T) is given by the following expression:

$$e_c = \frac{pt}{1+pt} + e_m t \quad .$$

The parameters c, p, and e_m are expressed in both the English and SI systems as follows:

English

$$\ln c = -1.350 - 5620.0/T - 0.05060\,\sigma + 1.9180 \ln \sigma \ ,$$
$$\ln p = 31.0 - 67310/T + 0.33060\,\sigma - 0.001885\,\sigma^2 \ ,$$
$$\ln e_m = 43.69 - 106400/T + 0.294\,\sigma + 2.596 \ln \sigma \ ,$$

where

T = degrees, Rankine,

σ = stress, ksi,

ln = natural logarithm.

SI

$$\ln c = -5.0530 - 3122/T - 0.007346\,\sigma + 1.918 \ln \sigma \ ,$$
$$\ln p = 31.0 - 37400/T + 0.04796\,\sigma - 3.965 \times 10^{-5}\,\sigma \ ,$$
$$\ln e_m = 38.68 - 59110/T + 0.04268\,\sigma + 2.596 \ln \sigma \ ,$$

where

T = degrees, Kelvin,

σ = stress, MPa,

e_c = strain, per cent,

t = time, hours.

TABLE V
COMPARISON OF COMPUTED HANGER FORCES[a]

Hanger Number[b]	Current Investigation	Elbow31[c] Model	Elbow31B[c] Model	MARC[c]	PISAC[d]	PINA[d]
1	15530 N	16630 N	17120 N	18180 N	20510 N	20530 N
	(3492 lbf)	(3738 lbf)	(3848 lbf)	(4087 lbf)	(4610 lbf)	(4615 lbf)
		+7.0%	+10.2%	+17.0%	+32.0%	+32.0%
2	24680 N	24420 N	24260 N	23310 N	23040 N	23620 N
	(5549 lbf)	(5490 lbf)	(5454 lbf)	(5240 lbf)	(5180 lbf)	(5310 lbf)
		-1.1%	-1.7%	-5.6%	-6.6%	-3.1%
3	24370 N	24480 N	24640 N	24550 N	24660 N	24070 N
	(5479 lbf)	(5503 lbf)	(5540 lbf)	(5519 lbf)	(5543 lbf)	(5502 lbf)
		+0.4%	+1.1%	+0.7%	+1.2%	-1.2%
4	25230 N	25130 N	25070 N	24950 N	24780 N	25570 N
	(5672 lbf)	(5649 lbf)	(5637 lbf)	(5609 lbf)	(5570 lbf)	(5502 lbf)
		-0.4%	-0.6%	-1.1%	-1.8%	-3.2%
5	27770 N	27590 N	26740 N	26890 N	27850 N	28450 N
	(6243 lbf)	(6202 lbf)	(6012 lbf)	(6046 lbf)	(6260 lbf)	(6395 lbf)
		-0.6%	-3.7%	-3.1%	-0.3%	+2.4%

[a] These forces were calculated in load step i of Table I.
[b] These numbers refer to Fig. 2.
[c] Results summarized in Ref. 2.
[d] Results summarized in Ref. 3.

DISTRIBUTION

	Copies
Nuclear Regulatory Commission, R7, Bethesda, Maryland	248
Technical Information Center, Oak Ridge, Tennessee	2
Los Alamos National Laboratory, Los Alamos, New Mexico	45
	295

NRC FORM 335 (6-83) U.S. NUCLEAR REGULATORY COMMISSION

BIBLIOGRAPHIC DATA SHEET

1 REPORT NUMBER (Assigned by TIDC and Vol. No. if any)
NUREG/CR-3845
LA-10090-MS

2 Leave blank

3 TITLE AND SUBTITLE
Prediction of Nonlinear Structural Response in LMFBR Elevated-Temperature Piping

4 RECIPIENT'S ACCESSION NUMBER

5 DATE REPORT COMPLETED
MONTH: March YEAR: 1984

6 AUTHOR(S)
Charles Farrar

7 DATE REPORT ISSUED
MONTH: June YEAR: 1984

8 PERFORMING ORGANIZATION NAME AND MAILING ADDRESS (Include Zip Code)
Los Alamos National Laboratory
Los Alamos, NM 87545

9 PROJECT/TASK/WORK UNIT NUMBER

10 FIN NUMBER
A7242

11 SPONSORING ORGANIZATION NAME AND MAILING ADDRESS (Include Zip Code)
Severe Accident Assessment Branch
Division of Accident Evaluation
Office of Nuclear Reactor Research
US Nuclear Regulatory Commission
Washington, DC 20555

12a TYPE OF REPORT
Informal

12b PERIOD COVERED (Inclusive dates)

13 SUPPLEMENTARY NOTES

14 ABSTRACT (200 words or less)

The development of structural analysis capabilities to investigate possible accident initiations caused by structural degradation of liquid metal fast breeder reactor (LMFBR) piping is summarized. The ABAQUS finite element code is used to perform a nonlinear analysis of a bench mark problem proposed by the Pressure Vessel Research Committee. The problem is representative both in geometry and loading of an LMFBR elevated-temperature piping system, and published analytical results are available for comparison. Results show the system to be most sensitive to large, radial, thermal gradients that occur when the system experiences certain thermal transients. Repeated cycles of these transients will lead to thermal ratcheting, causing progressive deformation and strain accumulation in the system. Future work will verify the accuracy of the finite element model and quantify damage accumulated during the lifetime of an LMFBR elevated-temperature piping system.

15a KEY WORDS AND DOCUMENT ANALYSIS

15b DESCRIPTORS

16 AVAILABILITY STATEMENT
Unlimited

17 SECURITY CLASSIFICATION (This report)
Unclassified

18 NUMBER OF PAGES

19 SECURITY CLASSIFICATION (This page)
Unclassified

20 PRICE
$

Available from

GPO Sales Program
Division of Technical Information and Document Control
US Nuclear Regulatory Commission
Washington, DC 20555

and

National Technical Information Service
Springfield, VA 22161

Los Alamos